

# Influence of the Covalent Heme–Protein Bonds on the Redox Thermodynamics of Human Myeloperoxidase

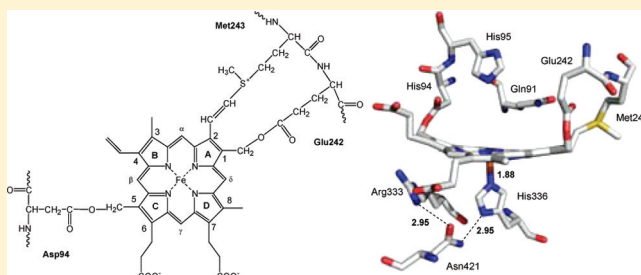
Gianantonio Battistuzzi,<sup>†</sup> Johanna Stampfer,<sup>‡</sup> Marzia Bellei,<sup>†</sup> Jutta Vlasits,<sup>‡</sup> Monika Soudi,<sup>‡</sup> Paul G. Furtmüller,<sup>‡</sup> and Christian Obinger<sup>\*,‡</sup>

<sup>†</sup>Department of Chemistry, University of Modena and Reggio Emilia, via Campi 183, 41100 Modena, Italy

<sup>‡</sup>Vienna Institute of BioTechnology, Department of Chemistry, Division of Biochemistry, BOKU-University of Natural Resources and Life Sciences, Muthgasse 18, A-1190 Vienna, Austria

**ABSTRACT:** Myeloperoxidase (MPO) is the most abundant neutrophil enzyme and catalyzes predominantly the two-electron oxidation of ubiquitous chloride to generate the potent bleaching hypochlorous acid, thus contributing to pathogen killing as well as inflammatory diseases. Its catalytic properties are closely related with unique posttranslational modifications of its prosthetic group. In MPO, modified heme *b* is covalently bound to the protein via two ester linkages and one sulfonium ion linkage with a strong impact on its (electronic) structure and biophysical and chemical properties.

Here, the thermodynamics of the one-electron reduction of the ferric heme in wild-type recombinant MPO and variants with disrupted heme–protein bonds (M243V, E242Q, and D94V) have been investigated by thin-layer spectroelectrochemistry. It turns out that neither the oligomeric structure nor the N-terminal extension in recombinant MPO modifies the peculiar positive reduction potential ( $E^\circ = 0.001$  V at 25 °C and pH 7.0) or the enthalpy or entropy of the Fe(III) to Fe(II) reduction. By contrast, upon disruption of the MPO–typical sulfonium ion linkage, the reduction potential is significantly lower ( $-0.182$  V). The M243V mutant has an enthalpically stabilized ferric state, whereas its ferrous form is entropically favored because of the loss of rigidity of the distal H-bonding network. Exchange of an adjacent ester bond (E242Q) induced similar but less pronounced effects ( $E^\circ = -0.094$  V), whereas in the D94V variant ( $E^\circ = -0.060$  V), formation of the ferrous state is entropically disfavored. These findings are discussed with respect to the chlorination and bromination activity of the wild-type protein and the mutants.



Heme peroxidases catalyze one- and two-electron oxidation reactions of a great diversity of inorganic and organic compounds with hydrogen peroxide. They are involved in manifold physiological reactions and are widely distributed among Bacteria, Archaea, and Eukarya. All currently available gene sequences of these metalloenzymes (May 2011, >6600 entries in data banks) can be phylogenetically divided into two superfamilies that arose independently [peroxidase-cyclooxygenase (formerly animal peroxidases) and peroxidase-catalase (formerly non-animal or bacterial, fungal, and plant peroxidases)] and three families (dyp-type peroxidases, heme haloperoxidases, and diheme peroxidases).<sup>1,2</sup>

The peroxidase-cyclooxygenase superfamily consists of seven subfamilies<sup>3</sup> with vertebrate (including mammalian) peroxidases (i.e., subfamily 1) playing an important role in biology, because they contribute to host defense against infection, hormone synthesis, and pathogenesis.<sup>4,5</sup> The most important structural feature of vertebrate heme peroxidases is the modification of the 1- and 5-methyl groups on pyrrole rings A and C of the heme group allowing formation of ester linkages with the carboxyl groups of a glutamate and an aspartate (Figure 1),<sup>6,7</sup> conserved in the four clades, myeloperoxidase (MPO), eosinophil peroxidase (EPO), lactoperoxidase (LPO), and thyroid peroxidase (TPO).<sup>8–13</sup> The clade of MPO is

unique in having a third covalent bond between the prosthetic group and the protein,<sup>3</sup> which connects the  $\beta$ -carbon of the vinyl group on pyrrole ring A with the sulfur atom of methionine 243, giving rise to an (electron-withdrawing) sulfonium ion linkage (Figure 1).<sup>8,9</sup> Formation of these covalent heme–protein bonds has been demonstrated to occur autocatalytically.<sup>12–16</sup>

The heme–protein covalent bonds have a deep impact on the biochemical and biophysical properties of mammalian peroxidases. In particular, they cause a distortion of the porphyrin ring from planarity, which is more pronounced in MPO<sup>8,9</sup> than in LPO.<sup>10</sup> In myeloperoxidase, the heme ring features a bow-shaped structure with less symmetry (Figure 1) and a considerably out-of-plane location of the high-spin iron ion, which are reflected by the peculiar UV–vis and resonance Raman spectral features of its ferric and ferrous states.<sup>7,17–20</sup> Importantly, the heme modification alters the chemistry of the prosthetic group, helping to protect it from (further) modification by catalytically generated reactive products of these enzymes,<sup>14–16</sup> which include (antimicrobial) hypohalous

**Received:** June 1, 2011

**Revised:** August 19, 2011

**Published:** August 19, 2011

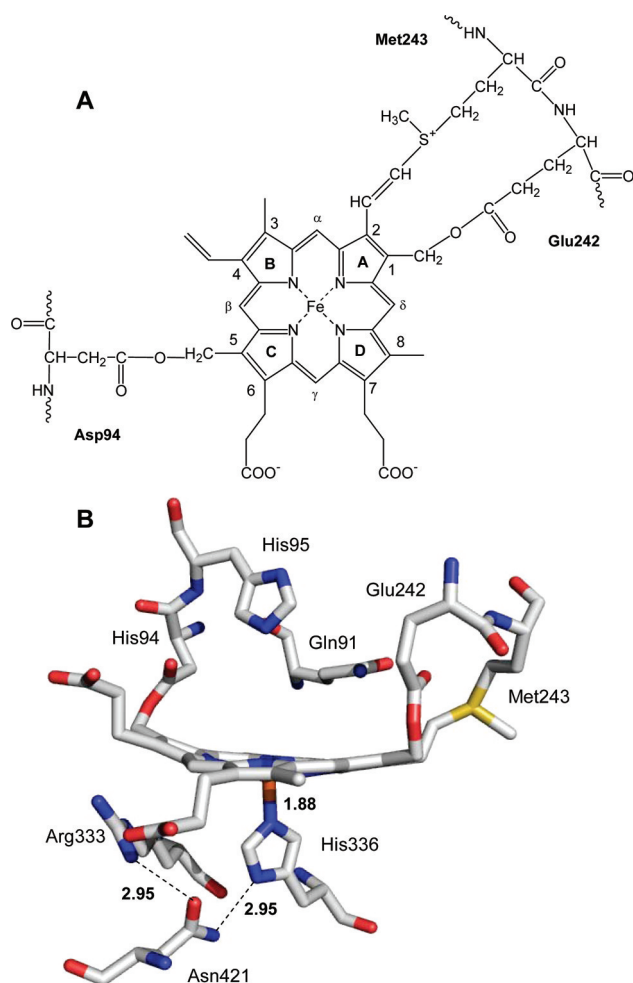


**Figure 1.** (A) Covalent binding pattern of heme in human myeloperoxidase. The ester linkages between the 1- and 5-methyl carbons and glutamate 242 and aspartate 94, respectively, are conserved in all vertebrate peroxidases. The sulfonium ion linkage between the sulfur atom of Met243 and the  $\beta$ -carbon of the pyrrole ring A vinyl group is present in only MPO. (B) Active site structure of human myeloperoxidase showing the amino acids involved in heme binding (D94, E242, and M243) as well as fully conserved distal and proximal residues. This figure was constructed using entry 3F9P of the Protein Data Bank.<sup>9</sup>

acids. On the other hand, this posttranslational modification modulates the redox chemistry by increasing the reduction potentials of the Fe(III)/Fe(II), compound I/Fe(III), and compound I/compound II couples, which provides the thermodynamic basis for the effective two-electron oxidation of halides, including bromide and chloride.<sup>21</sup> For example, the reduction potentials of the Fe(III)/Fe(II) couple of LPO and EPO are  $-176$  and  $-126$  mV, respectively,<sup>22</sup> whereas it is positive in MPO ( $5$  mV).<sup>23</sup> The extraordinary high (globin-like) reduction potential and the sulfonium ion linkage, whose positive charge and electron withdrawing effect stabilize the ferrous form of the enzyme, have been related to the unique ability of myeloperoxidase to oxidize chloride.<sup>24,25</sup> Additionally, the two ester linkages have also been shown to influence the biophysical and enzymatic properties of MPO.<sup>26,27</sup>

To improve our understanding of the relationship between heme modification and redox chemistry in MPO, a comprehensive spectroelectrochemical investigation of redox properties of recombinant wild-type MPO (recMPO) and its

M243V, E242Q, and D94V variants, in which the covalent heme–protein bonds have been selectively removed, was performed. The relative contribution of the three covalent bonds to the reduction potential of the Fe(III)/Fe(II) couple in MPO as well as to the enthalpy and entropy changes accompanying the reduction reaction is presented and discussed with respect to the known spectral and enzymatic features of the variants. Obtained data are compared with those available for homologous EPO and LPO and peroxidases with noncovalently linked heme.

## MATERIALS AND METHODS

Transfection of recombinant plasmids into Chinese hamster ovary cells, selection, culture procedures, and protein purification protocols were described previously.<sup>25–28</sup> Concentrations of wild-type recombinant MPO (recMPO) and its D94V, E242Q, and M243V variants were determined spectrophotometrically by using extinction coefficients of  $91 \text{ mM}^{-1} \text{ cm}^{-1}$  at  $430 \text{ nm}$ ,<sup>29</sup>  $72 \text{ mM}^{-1} \text{ cm}^{-1}$  at  $428 \text{ nm}$ ,<sup>27</sup>  $85 \text{ mM}^{-1} \text{ cm}^{-1}$  at  $418 \text{ nm}$ ,<sup>26</sup> and  $84 \text{ mM}^{-1} \text{ cm}^{-1}$  at  $412 \text{ nm}$ ,<sup>25</sup> respectively. The purity indices ( $\text{Reinheitszahl}$ ,  $A_{\text{Soret}}/A_{280}$ ) of the wild-type recombinant protein and its variants varied from  $0.54$  to  $0.71$ ,<sup>25–27</sup> with  $\sim 0.72$  (recMPO) reflecting 100% heme occupancy.

**Spectroelectrochemistry.** All experiments were conducted in a homemade OTTLE cell.<sup>30–32</sup> The three-electrode configuration consisted of a gold minigrad working electrode (Buckbee-Mears, Chicago, IL), a homemade Ag/AgCl/KCl<sub>sat</sub> microreference electrode, separated from the working solution by a Vycor set, and a platinum wire as the counter electrode. The reference electrode was calibrated against a saturated calomel electrode before each set of measurements. All potentials are referenced to the standard hydrogen electrode (SHE). Potentials were applied across the OTTLE cell with an Amel model 2053 potentiostat/galvanostat. The functioning of the OTTLE cell was checked by measuring the reduction potential of yeast iso-1-cytochrome *c* under conditions similar to those used in this work. The  $E^{\circ'}$  value corresponded to that determined by cyclic voltammetry ( $260 \text{ mV}$ ). The constant temperature was maintained by a circulating water bath, and the OTTLE cell temperature was monitored with a Cu-costan microthermocouple. UV–vis spectra were recorded using a Varian Cary C50 spectrophotometer.

The variable-temperature experiments were performed using a “non-isothermal” cell configuration, in which the temperature of the reference electrode and the counter electrode was kept constant, while that of the working electrode was varied. For this experimental configuration,  $\Delta S^{\circ'}_{\text{rc}}$  is calculated from the slope of the  $E^{\circ'}$  versus temperature plot, whereas  $\Delta H^{\circ'}_{\text{rc}}$  is obtained from the Gibbs–Helmholtz equation,  $\Delta G^{\circ'}_{\text{rc}} = \Delta H^{\circ'}_{\text{rc}} - T\Delta S^{\circ'}_{\text{rc}} = -nFE^{\circ'}$  (where  $F$  is the Faraday constant and  $n$  represents the number of electrons transferred by the redox couple), namely from the slope of the  $E^{\circ'}/T$  versus  $1/T$  plot.<sup>33</sup>

The spectroelectrochemical experiments were conducted under argon from  $10$  to  $40^\circ\text{C}$ . The following mediators were used: (i)  $20 \mu\text{M}$  *N,N,N',N'*-tetramethylphenylenediamine, 2-hydroxy-1,4-naphthoquinone, phenazine methosulfate, and phenazine ethosulfate for recMPO and the D94V and E242Q variants and (ii)  $10 \mu\text{M}$  methyl viologen and  $1 \mu\text{M}$  lumiflavine 3-acetate, indigo disulfonate, phenazine methosulfate, and methylene blue for the M243V mutant. In a typical experiment,  $1 \text{ mL}$  samples were used, containing  $4.5 \mu\text{M}$  MPO in  $0.1 \text{ M}$  phosphate buffer and  $0.1 \text{ M}$  NaCl ( $\text{pH } 7$ ). Nernst plots

consisted of at least five points and were invariably linear, with a slope consistent with a one-electron reduction process.

## RESULTS

The electronic spectra of ferric high-spin monomeric wild-type recombinant MPO (recMPO) and its M243V, E242Q, and D94V variants recorded at different applied potentials in the OTTLE cell (25 °C, pH 7) are reported in Figures 2 and 3,

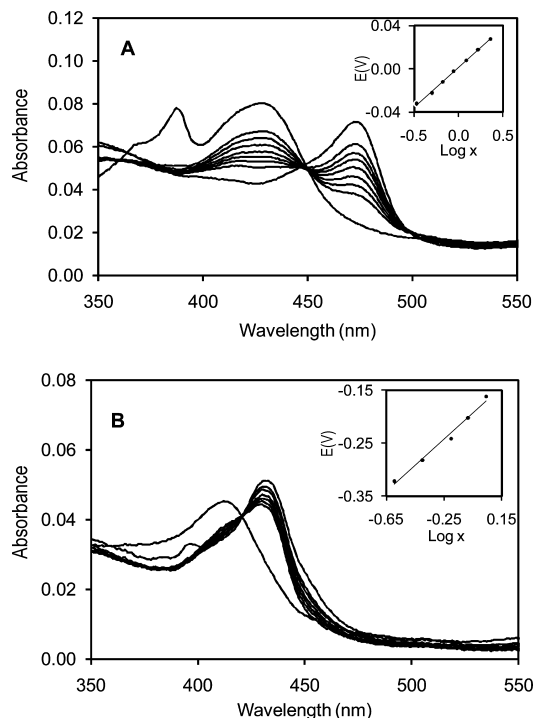


**Figure 2.** Electronic spectra of (A) high-spin recombinant wild-type MPO and (B) the high-spin recombinant M243V mutant obtained at various potentials in spectroelectrochemical experiments conducted with an OTTLE cell at 25 °C. The corresponding Nernst plots are reported in the insets, where  $X$  represents  $[(A_{\lambda_{\text{red}}}^{\text{max}} - A_{\lambda_{\text{red}}}) / (A_{\lambda_{\text{ox}}}^{\text{max}} - A_{\lambda_{\text{ox}}})]$  and  $\lambda_{\text{ox}} = 430$  nm and  $\lambda_{\text{red}} = 473$  nm and  $\lambda_{\text{ox}} = 412$  nm and  $\lambda_{\text{red}} = 434$  nm for recombinant wild-type MPO and the M243V mutant, respectively.

respectively. Upon reduction, direct conversion of ferric forms of recMPO and the D94V and E242Q mutants to the corresponding ferrous species was observed. Reduction of ferric M243V proceeds through the formation of a transient ferrous intermediate with band maxima at 444 nm (Soret band), 561 nm, and 593 nm, which was not stable but converted slowly within 45–60 min into a new stable Fe(II) form, characterized by absorption maxima at 434 nm (Soret band), 561 nm, and 593 nm, respectively. A similar behavior has been observed for LPO.<sup>20,22</sup> Thus, to avoid any interference from the transient Fe(II) intermediate, the M243V MPO mutant was first fully reduced electrochemically, allowing its complete conversion into the stable ferrous form, which was then subjected to (oxidative) spectroelectrochemical titrations, as in the case of LPO.<sup>20,22</sup> Therefore, the  $E^{\circ}$  values and the corresponding reduction thermodynamics refer to the redox equilibrium between the stable Fe(II) form of the M243V mutant and the ferric species.

The Nernst plots obtained from the spectroelectrochemical titrations are invariably linear (insets of Figures 2 and 3) with

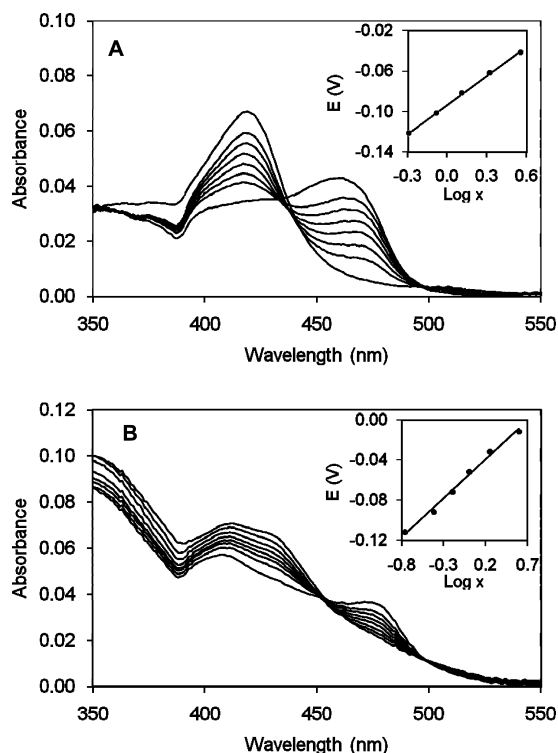


**Figure 3.** Electronic spectra of (A) high-spin E242Q and (B) high-spin D94V MPO mutants obtained at various potentials in spectroelectrochemical experiments conducted with an OTTLE cell at 25 °C. The corresponding Nernst plots are reported in the insets, where  $X$  represents  $[(A_{\lambda_{\text{red}}}^{\text{max}} - A_{\lambda_{\text{red}}}) / (A_{\lambda_{\text{ox}}}^{\text{max}} - A_{\lambda_{\text{ox}}})]$  and  $\lambda_{\text{ox}} = 418$  nm and  $\lambda_{\text{red}} = 460$  nm and  $\lambda_{\text{ox}} = 428$  nm and  $\lambda_{\text{red}} = 475$  nm for the E242Q and D94V mutants, respectively.

slopes close to the theoretical value of  $RT/F$  (0.059 V) at 25 °C, as expected for the one-electron reduction process. For recMPO, the calculated standard reduction potential  $\{E^{\circ}[\text{Fe(III)/Fe(II)}]\}$  is 0.001 V ( $\pm 0.005$  V) and coincides, within experimental error, with that of native dimeric myeloperoxidase isolated from leukocytes<sup>23</sup> (Table 1). On the other hand, the  $E^{\circ}$  values for M243V ( $-0.182 \pm 0.005$  V), E242Q ( $-0.094 \pm 0.005$  V), and D94V ( $-0.055 \pm 0.005$  V) are significantly lower than that of recMPO (Table 1), explicitly demonstrating the influence exerted by the covalent heme–protein linkages on the redox properties of the prosthetic group.

The temperature profiles of the  $E^{\circ}$  values for recMPO and its M243V, E242Q, and D94V variants are shown in Figure 4, together with that of native MPO.<sup>23</sup> The spectroelectrochemical response deteriorates above 35–40 °C because of protein denaturation and solvent evaporation. The obtained temperature profiles allowed factorization of the enthalpy ( $\Delta H^{\circ}_{\text{rc}}$ ) and entropy ( $\Delta S^{\circ}_{\text{rc}}$ ) changes during the reduction reaction (Table 1). It turns out that the reduction thermodynamics of recMPO are almost coincident, within experimental error, with those of the native leukocyte protein, whereas mutation of M243, E242, or D94 alters the corresponding  $\Delta H^{\circ}_{\text{rc}}$  and  $\Delta S^{\circ}_{\text{rc}}$  values. In particular, the selective disruption of the individual heme–protein linkages invariably induces opposing effects of the reduction thermodynamics of the Fe(III)/Fe(II) couple (Table 1); i.e., the mutation-induced changes in  $\Delta H^{\circ}_{\text{rc}}$  and  $\Delta S^{\circ}_{\text{rc}}$  partially offset each other. The existence of this enthalpy–entropy compensation indicates that both reduction enthalpy and entropy are sensibly influenced by reduction-induced



**Table 1. Thermodynamic Parameters for the Fe(III) → Fe(II) Reduction in Wild-Type Recombinant Myeloperoxidase (recMPO) and Mutants with Disrupted Heme–Protein Bonds<sup>a</sup>**

protein	$E^{\circ}$ (V)	$\Delta H^{\circ}_{rc}$ (kJ/mol)	$\Delta S^{\circ}_{rc}$ (J K <sup>-1</sup> mol <sup>-1</sup> )	$\Delta H^{\circ}_{rc}(\text{int}) (= \Delta G^{\circ} = -nFE^{\circ})$ (kJ/mol)
recMPO	0.001	−1	−3	0
M243V	−0.182	37	62	18
E242Q	−0.094	24	49	9
D94V	−0.055	−2	−14	5
MPO	0.005	3	10	0
EPO	−0.126	7	−18	12
LPO	−0.176	−5	−73	17

<sup>a</sup>For comparison, thermodynamic data of dimeric leukocyte myeloperoxidase (MPO)<sup>23</sup> and homologous lactoperoxidase (LPO) and eosinophil peroxidase (EPO)<sup>22</sup> are shown. Errors for  $E^{\circ}$ ,  $\Delta H^{\circ}_{rc}$  and  $\Delta S^{\circ}_{rc}$  are  $\pm 0.005$  V,  $\pm 4$  kJ/mol, and  $\pm 8$  J K<sup>-1</sup> mol<sup>-1</sup>, respectively (calculated from the upper value of the standard deviation of the least-squares fits of the data points within the series). The standard reduction potential  $E^{\circ}$  is measured at 298.15 K and referred to the SHE. Please note that often the sum  $(-\Delta H^{\circ}_{rc}/F + T_{298}\Delta S^{\circ}_{rc}/F)$  does not exactly match  $E^{\circ}$  because the  $\Delta H^{\circ}_{rc}$  and  $\Delta S^{\circ}_{rc}$  values are rounded to the closest integer, as a result of experimental error.

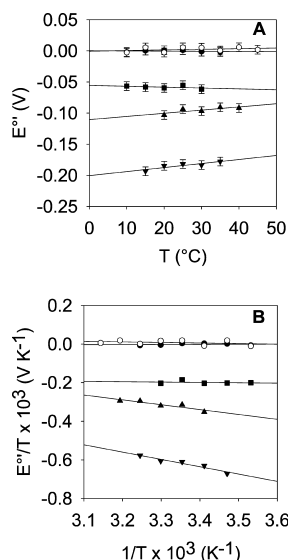


**Figure 4.** Temperature dependence of the reduction potential (A) and  $E^{\circ}/T$  vs  $1/T$  (B) for native leukocyte MPO (○), recombinant MPO (●), and its M243V (▼), E242Q (▲), and D94V (■) mutants. The slopes of the plots yield  $\Delta S^{\circ}_{rc}/F$  and  $-\Delta H^{\circ}_{rc}/F$ , respectively. Solid lines are least-squares fits to the data points. When not visible, error bars have the same dimensions as the symbols. The data for native leukocyte MPO were taken from ref 23.

solvent reorganization effects. Hence,  $\Delta H^{\circ}_{rc}$  and  $\Delta S^{\circ}_{rc}$  can be partitioned into intrinsic protein contributions ( $\Delta H^{\circ}_{rc,\text{int}}$  and  $\Delta S^{\circ}_{rc,\text{int}}$  respectively) and solvent reorganization factors ( $\Delta H^{\circ}_{rc,\text{solv}}$  and  $\Delta S^{\circ}_{rc,\text{solv}}$  respectively) with  $\Delta H^{\circ}_{rc} = \Delta H^{\circ}_{rc,\text{int}} + \Delta H^{\circ}_{rc,\text{solv}}$  and  $\Delta S^{\circ}_{rc} = \Delta S^{\circ}_{rc,\text{int}} + \Delta S^{\circ}_{rc,\text{solv}}$ .<sup>30–36</sup>

$\Delta H^{\circ}_{rc,\text{int}}$  depends mainly on the donor properties of the axial heme ligands, the polarity of the protein environment, and the electrostatic interactions between the redox center and polar and charged residues surrounding the heme, whereas  $\Delta S^{\circ}_{rc,\text{int}}$  is related to the redox state-dependent differences in protein flexibility.<sup>30–36</sup> Because reduction-induced overall structural changes are quite small in heme-bound proteins, the measured  $\Delta S^{\circ}_{rc}$  is generally attributed, as a first approximation, to reduction-induced solvent reorganization effects only, thereby neglecting the contribution from conformational changes in the protein (i.e.,  $\Delta S^{\circ}_{rc,\text{int}} \approx 0$ ).<sup>30–36</sup> This approach proved to be correct for native MPO,<sup>23</sup> LPO and EPO,<sup>22</sup> and heme peroxidases from the peroxidase-catalase superfamily (HRP,<sup>34</sup> ARP,<sup>32</sup> and KatG<sup>31</sup>). Hence, to a first approximation, for

recMPO and variants M243V, E242Q, and D94V,  $\Delta S^{\circ}_{rc} = \Delta S^{\circ}_{rc,\text{solv}} = -3, 62, 49$ , and  $-14$  J K<sup>-1</sup> mol<sup>-1</sup>, respectively (Table 1).

Because reduction-induced solvent reorganization effects generate compensatory enthalpy and entropy changes,<sup>30,33,36</sup> the related enthalpic contribution can be factorized out from the measured enthalpy change, allowing estimation of the protein-based contribution to  $\Delta H^{\circ}_{rc}$ :  $\Delta H^{\circ}_{rc,\text{int}} = \Delta H^{\circ}_{rc} - \Delta H^{\circ}_{rc,\text{solv}} = \Delta H^{\circ}_{rc} - T\Delta S^{\circ}_{rc} = \Delta G^{\circ}_{rc} = -nFE^{\circ}$  ( $n = 1$ ). Therefore, to a first approximation, the reduction potential is determined by the selective enthalpic stabilization of one of the two redox states by first-coordination sphere and electrostatic effects. For recMPO and its three variants,  $\Delta H^{\circ}_{rc,\text{int}} = -nFE^{\circ}$ , which corresponds to 0 kJ/mol (recMPO), 18 kJ/mol (M243V), 9 kJ/mol (E242Q), and 5 kJ/mol (D94V) (Table 1).

## DISCUSSION

Heme proteins conduct a myriad of different biological functions, including oxygen transport, storage and reduction, electron transfer, and redox catalysis. Thus, it is challenging to investigate and understand the role of (posttranslational) modifications of the prosthetic group and/or of its protein environment in fine-tuning of biophysical and biochemical features of these oxidoreductases. Although not directly involved in the catalytic cycle, the redox behavior of the Fe(III)/Fe(II) couple in heme peroxidases has been analyzed in a much greater detail than that of the short-living high-potential compound I and compound II,<sup>36</sup> whose reduction potentials are more difficult to measure experimentally. Nevertheless, there is a general agreement that the molecular factors that determine  $E^{\circ}[\text{Fe(III)/Fe(II)}]$  influence also  $E^{\circ}$  of the catalytically relevant compound I/Fe(III) and compound I/compound II redox couples.<sup>7,36</sup> Indeed, the hierarchy observed for  $E^{\circ}[\text{Fe(III)/Fe(II)}]$ , namely, MPO > EPO > LPO, is also reflected in  $E^{\circ}[\text{compound I/Fe(III)}]$  and  $E^{\circ}[\text{compound I/compound II}]$ .<sup>21,36</sup>

Myeloperoxidase is unique because it is the only human oxidoreductase that is able to oxidize chloride at reasonable rates, and the thermodynamic basis for this reactivity is related to its peculiar redox properties. In contrast to other heme peroxidases, which feature  $E^{\circ}[\text{Fe(III)/Fe(II)}]$  values between  $-0.125$  and  $-0.320$  V (to stabilize the ferric state for efficient reaction with  $\text{H}_2\text{O}_2$ ),<sup>36</sup> the corresponding reduction potential in dimeric leukocyte MPO is  $0.005$  V<sup>23</sup> or  $0.001$  V in the monomeric recombinant protein at pH 7.0 and 25 °C (Table 1).

**Table 2. Overall Halogenation Activity (units per milligram) and Apparent Bimolecular Rate Constants of Compound I Reduction by Chloride and Bromide of Wild-Type recMPO and Variants M243V,<sup>25</sup> E242Q,<sup>26</sup> and D94V<sup>27</sup> in 100 mM Phosphate Buffer at pH 7.0 and 25 °C<sup>a</sup>**

protein		chloride	bromide
wild-type recMPO <sup>b</sup>	units/mg	0.893 (100%)	5.62 (100%)
	compound I reduction ( $\times 10^4$ M <sup>-1</sup> s <sup>-1</sup> )	3.6 (100%)	140 (100%)
M243V	units/mg	0.017 (1.9%)	0.71 (12.6%)
	compound I reduction ( $\times 10^4$ M <sup>-1</sup> s <sup>-1</sup> )	nr	13 (9.3%)
E242Q	units/mg	0.029 (3.3%)	2.14 (38%)
	compound I reduction ( $\times 10^4$ M <sup>-1</sup> s <sup>-1</sup> )	0.0065 (0.2%)	5.4 (3.9%)
D94V	units/mg	0.45 (12.6%)	40.7 (29.1%)
	compound I reduction ( $\times 10^4$ M <sup>-1</sup> s <sup>-1</sup> )	0.15 (4.2%)	41 (29.3%)
LPO	units/mg	0.027 (3.0%)	0.33 (5.8%)
	compound I reduction ( $\times 10^4$ M <sup>-1</sup> s <sup>-1</sup> )	nr	4.1 (2.9%)

<sup>a</sup>For comparison, data for lactoperoxidase (LPO) are included. The reference (100%) is wild-type recombinant MPO (recMPO). One unit is defined as halogenation of 1  $\mu$ mol of monochlorodimedone per minute at 25 °C. nr means no reaction. <sup>b</sup>Compound I reduction rates of native dimeric MPO<sup>6,21</sup> from leukocytes are very similar to those presented here for recombinant monomeric MPO.

The globin-like reduction potential of homodimeric MPO and monomeric recMPO is due to the small  $\Delta H'^{\circ}_{\text{rc}}$  and  $\Delta S'^{\circ}_{\text{rc}}$  values, which almost perfectly offset each other (Table 1). The sulfonium ion linkage drastically decreases the level of enthalpic stabilization of the ferric form compared to those of the other mammalian heme peroxidases (LPO and EPO). In fact, the positive charge of the sulfur atom electrostatically destabilizes the ferric heme, which features a +1 charge at its core (compared to the uncharged ferrous form). Moreover, the electron withdrawing effect of the sulfonium ion linkage reduces the basicity of the four pyrrole nitrogens, thereby decreasing the electron density at the heme iron. Additionally, this effect might be enhanced by the pronounced distortion of the porphyrin ring, which further weakens the interaction of the pyrrole nitrogens with the iron ion,<sup>7–9,23</sup> as recently reported for the nitric oxide/oxygen binding (H-NOX) heme protein from *Thermoanaerobacter tengcongensis*, which contains a H<sub>2</sub>O(OH<sup>-</sup>) six-coordinate heme.<sup>37,38</sup> This view is supported by a recent DFT study,<sup>39</sup> which indicated that a distorted porphyrin ring features a weaker  $\pi$ -conjugation with the iron compared to a planar porphyrin ring, resulting in destabilization of the ferric state. However, it is important to stress that many other studies of heme proteins and model systems indicate that lowering the level of heme distortion increases  $E'^{\circ}$ .<sup>40–42</sup> This clearly demonstrates that the effect of distortion of the heme on  $E'^{\circ}[\text{Fe(III)/Fe(II)}]$  can be influenced by several other factors, including axial ligation.<sup>40</sup>

On the other hand, the small  $\Delta S'^{\circ}_{\text{rc}}$  suggests that Fe(III) reduction is accompanied by limited solvent reorganization, indicating that the hydrogen bond network of water molecules in the substrate channel leading to the distal heme site is quite rigid. The low mobility of the water molecules in the heme distal cavity has been proposed to be crucial in fixing the position of the chloride and in helping in the transfer and incorporation of the oxyferryl oxygen into HClO.<sup>23</sup>

Recombinant monomeric MPO shares almost identical spectral and enzymatic features with the mature dimeric leukocyte enzyme.<sup>19,20,24–29,43</sup> This work demonstrates that this similarity extends also to  $E'^{\circ}$ ,  $\Delta H'^{\circ}_{\text{rc}}$  and  $\Delta S'^{\circ}_{\text{rc}}$  of the Fe(III)/Fe(II) couple, which coincide within experimental error (Table 1). Because (i)  $\Delta H'^{\circ}_{\text{rc,int}}$  is determined by metal–ligand interactions and the electrostatics at the interface among the metal, the protein environment, and the solvent and (ii)  $\Delta S'^{\circ}_{\text{rc}}$  mainly represents reduction-induced solvent

reorganization effects,<sup>23,36</sup> it can be concluded that differences in the overall structure do not affect the electronic and solvation properties of the heme cavity. This is important, because the designed variants investigated in this work correspond to the monomeric form produced in CHO cells. Mature leukocyte MPO is a glycosylated homodimer with each monomer consisting of a light chain and a heavy chain that both contribute to binding of the modified heme. By contrast, because of the fact that biosynthesis in CHO cells lacks some proteolytic steps, recMPO is monomeric, contains an N-terminal propeptide (thus often designated as proMPO), and differs in glycan structure and conformational and thermal stability.<sup>44,45</sup> It must be noted that a monomeric proMPO form has been shown to be released also by disruption of the Golgi due to the treatment of cultured promyelocytes with brefeldin A<sup>46</sup> or by foam cells newly engaged in MPO gene transcription by local cytokines.<sup>47</sup> It is reasonable to assume that these MPO forms have a similar architecture of both the heme cavity and the substrate access channel.

**Sulfonium Ion Linkage.** Upon disruption of the sulfonium ion linkage in the M243V variant, the Soret band (412 nm) and additional absorption maxima (500, 545, 586, and 635 nm) were considerably blue-shifted (Figure 2B) and similar to those found in EPO and LPO.<sup>6,11,20,24,25</sup> The resonance Raman (RR) spectrum of MPO M243V has been shown to resemble very closely that of LPO, indicating a less constrained heme.<sup>19,20</sup> This similarity is also underlined by the fact that ferrous wild-type MPO is stable between pH 5 and 8.5,<sup>20</sup> whereas reduction of LPO and the MPO variant M243V gives rise to two Fe(II) forms.<sup>20</sup>

Besides spectral similarities, LPO and MPO M243V share negligible chlorination and low bromination activity (Table 2),<sup>25</sup> and this work supports the hypothesis that these enzymatic properties are based on comparable reduction potentials. Data of apparent bimolecular rate constants of compound I reduction by either chloride or bromide presented in Table 2 also demonstrate that differences in  $E'^{\circ}$  values of the Fe(III)/Fe(II) couple are reflected by differences in  $E'^{\circ}$  values of the compound I/Fe(III) couple.

In MPO M243V, the measured  $E'^{\circ}$  value (−0.182 V) is significantly lower than that of the recombinant wild-type protein and almost identical to that of LPO (Table 1).<sup>22</sup> Moreover, exchange of M243 drastically increased  $\Delta H'^{\circ}_{\text{rc,int}}$  [ $\Delta\Delta H'^{\circ}_{\text{rc,int}}(\text{variant} - \text{recMPO}) = 18$  kJ/mol] (Table 1),

indicating that protein intrinsic factors enthalpically stabilize the oxidized form more efficiently than recMPO. This is in agreement with the effects of disruption of the sulfonium linkage, because deletion of the (positive and electron-withdrawing) bond should stabilize the ferric form of the heme both electrostatically and electronically.

Furthermore, deletion of methionine 243 induced a drastic increase in  $\Delta S^{\circ}_{\text{rc,solv}}$  [ $\Delta\Delta S^{\circ}_{\text{rc,solv}}(\text{variant-recMPO}) = 65 \text{ J K}^{-1} \text{ mol}^{-1}$ ], demonstrating that Fe(III) reduction in the variant is entropically favored, as a consequence of a significant reduction-induced solvent reorganization within the heme cavity not observed in wild-type recMPO or leukocyte MPO. This finding is in agreement with the proposed role of the sulfonium group in fixing the position of  $\text{H}_2\text{O}$  molecules in the distal heme cavity and in positioning of the anionic electron donor molecules (halide ions).<sup>6–9,23</sup> On the other hand, the lower solvent order in ferrous M243V reflects the weakened electrostatic interactions of the water molecules with the Fe(II) heme (overall core charge of 0) compared to that of Fe(III) heme (overall core charge of +1), as already observed in HRP-C.<sup>34</sup>

**Heme–Protein Ester Bonds.** The two heme–protein ester bonds are found in all vertebrate heme peroxidases, including LPO and EPO. The  $E^{\circ}$  value of MPO variant E242Q was determined to be  $-0.094 \text{ V}$  (Figure 3A and Table 1),  $0.095 \text{ V}$  lower than that of recMPO. Therefore, disruption of the ester bond at pyrrole ring A induced a sensible increase in protein-based enthalpic stabilization of the oxidized form [ $\Delta\Delta H^{\circ}_{\text{rc,int}}(\text{variant-recMPO}) = 9 \text{ kJ/mol}$ ], which, however, is lower than that observed in MPO M243V. Because in the E242Q mutant the sulfonium linkage is still present,<sup>26</sup> the observed effect is not related to electrostatics. Although the influence of heme distortion on the reduction potential of the heme iron is still controversial and not fully understood,<sup>37–42</sup> it is possible that the decreased level of distortion of the heme compared to that of recMPO enhances the interaction of the metal ion with the pyrrole nitrogens, thereby enthalpically stabilizing the ferric form. Reduction of E242Q is entropically favored [ $\Delta\Delta S^{\circ}_{\text{rc}}(\text{variant-recMPO}) = 52 \text{ J K}^{-1} \text{ mol}^{-1}$ ], which is in agreement with the hypothesis that E242 (besides M243) is important in fixing the position of the  $\text{H}_2\text{O}$  molecules in the distal heme cavity and optimizing the positioning of the anionic substrates (halide ions).<sup>26</sup> Indeed, the glutamate 242–heme ester bond is close to the bromide binding site in MPO,<sup>8</sup> and its disruption generally decreased the halogenation activity of E242Q compared to that of the wild-type protein (Table 2).<sup>26</sup> In fact, the observed  $\Delta\Delta S^{\circ}_{\text{rc}}$  indicates an increased level of reduction-induced solvent reorganization and a greater solvent mobility within the heme site compared to that of recMPO, as well as a lower solvent order in the ferrous form. Interestingly, the (positive)  $\Delta\Delta S^{\circ}_{\text{rc}}$  is smaller than that observed with MPO M243V, in agreement with the presence of the sulfonium linkage,<sup>26</sup> which should decrease the level of reduction-induced solvent reorganization compared to that of the mutant described above, because the water molecules electrostatically interact with both the ferrous (overall charge of +1) and ferric (overall charge of +2) forms of the heme.

The standard reduction potential of the Fe(III)/Fe(II) couple of the D94V mutant was determined to be  $-0.055 \text{ V}$ , sensibly lower than that of wild-type recMPO ( $\Delta E^{\circ} = -0.056 \text{ V}$ ) but higher than that of M243V ( $\Delta E^{\circ} = 0.127 \text{ V}$ ) or E242Q ( $\Delta E^{\circ} = 0.039 \text{ V}$ ). Elimination of this ester bond increases  $\Delta H^{\circ}_{\text{rc,int}}$  [ $\Delta\Delta H^{\circ}_{\text{rc,int}}(\text{variant-recMPO}) = 5 \text{ kJ/mol}$ ], demon-

strating that protein intrinsic factors enthalpically stabilize the oxidized form more efficiently than in recMPO, which again might reflect the less pronounced distortion of the prosthetic group in D94V compared to that in wild-type recMPO or leukocyte MPO.<sup>19</sup>

Disruption of the ester bond at pyrrole ring C (Figure 1) decreases  $\Delta S^{\circ}_{\text{rc}}$  [ $\Delta\Delta S^{\circ}_{\text{rc}}(\text{variant-recMPO}) = -11 \text{ J K}^{-1} \text{ mol}^{-1}$ ], showing that reduction of ferric D94V is entropically unfavored. This effect is opposite to that observed in the other mutants and much smaller in absolute value (Table 1), suggesting that this heme–ester bond plays a minor role in stabilization of the rigid H-bonding network at the distal heme site. This is in agreement with the observation that the halide binding (and oxidation) site is close to the  $\delta$ -meso bridge and the E242–heme bond (Figure 1) and thus almost opposite to D94.<sup>6,8,9</sup> The observed negative reduction entropy could be related to the destabilization of the  $\text{Ca}^{2+}$  binding site at the distal heme cavity that involves D96 in the proximity of D94 and catalytic H95 (Figure 1). Hence, it is reasonable to assume that disruption of the ester bond at pyrrole ring C increases the mobility of the polypeptide, including the V94–H95–D96 segment in the D94V variant (Figure 1). In any case, exchange of D94 slowed the chlorination and bromination reaction (Table 2),<sup>27</sup> suggesting also that this ester bond contributes to the high oxidation capacity of MPO.

In summary, this study clearly demonstrates that the large difference between the  $E^{\circ}$  values of MPO and LPO/EPO<sup>22</sup> ( $\sim 180$  and  $\sim 130 \text{ mV}$ , respectively) is mainly due to the presence of the positively charged electron-withdrawing sulfonium ion bond with a probable contribution of the pronounced heme distortion,<sup>8,9</sup> because the proximal histidine–asparagine interaction has been shown to be similar in all vertebrate peroxidases.<sup>7,9,20</sup> As a consequence, disruption of the MPO–typical sulfonium bond rendered the  $E^{\circ}$  value of the M243V mutant similar to that of LPO. It is very likely that the molecular factors determining  $E^{\circ}$  of the Fe(III)/Fe(II) couple influence the reduction potential of the catalytically relevant compound I/ferric MPO redox couple. Therefore, it is reasonable to assume that  $E^{\circ}[\text{compound I/Fe(III)}]$  of MPO M243V is also significantly lower than that of wild-type MPO ( $1160 \text{ mV}^{48,49}$ ), thus leading to an almost complete loss of chlorination [ $E^{\circ}(\text{HOCl/Cl}^{-}, \text{H}_2\text{O}) = 1230 \text{ mV}^{21}$ ] and a significant decrease in bromination activity [ $E^{\circ}(\text{HOBr/Br}^{-}, \text{H}_2\text{O}) = 1130 \text{ mV}^{21}$ ].<sup>24,25</sup>

Additionally, the redox properties of the E242Q and D94V mutants suggest that distortion of the heme from planarity, induced by the two corresponding heme–protein ester bonds, contributes to the increase in the  $E^{\circ}[\text{Fe(III)/Fe(II)}]$  of mammalian peroxidases (in particular LPO and EPO) compared to those of heme peroxidases with unmodified heme *b*, although to a smaller extent than the positively charged electron-withdrawing sulfonium ion linkage.

These data, which are supported by a recent density functional study,<sup>50</sup> nicely demonstrate how posttranslational modifications may alter the redox chemistry of the heme to meet a specific physiological demand, which in the case of MPO is binding and oxidation of chloride.

## AUTHOR INFORMATION

### Corresponding Author

\*Phone: +43-1-47654-6073. Fax: +43-1-47654-6059. E-mail: christian.obinger@boku.ac.at.



## Funding

This work was supported by the Austrian Science Fund (Project FWF P20664 and W1224, International Ph.D. program BioToP, Biomolecular Technology of Proteins), by the Ministero dell'Università e della Ricerca Scientifica (MUR) of Italy (Programmi di Ricerca Scientifica di Rilevante Interesse Nazionale 2007 Prot. n. 2007KAWXCL\_001), and by the University of Modena and Reggio Emilia (Fondo di Ateneo per la Ricerca, 2009).

## ABBREVIATIONS

MPO, myeloperoxidase; LPO, lactoperoxidase; EPO, eosinophil peroxidase; TPO, thyroid peroxidase; KatG, catalase-peroxidase from *Synechocystis* PCC6803; ARP, *Arthromyces ramosus* peroxidase; HRP-C, horseradish peroxidase isoform C;  $E^\circ$ , reduction potential, referenced to the standard hydrogen electrode, measured at pH 7.0;  $\Delta H^\circ_{\text{rc}}$ , enthalpy change for the reaction center upon reduction of the oxidized protein;  $\Delta S^\circ_{\text{rc}}$ , entropy change for the reaction center upon reduction of the oxidized protein; SHE, standard hydrogen electrode; ET, electron transport; CHO, Chinese hamster ovary; OTTLE, optical thin-layer electrochemistry.

## REFERENCES

- (1) Zamocky, M., and Obinger, C. (2010) Molecular phylogeny of heme peroxidases. In *Biocatalysis based on heme peroxidases* (Torres, E., and Ayala, M., Eds.) pp 7–30, Springer-Verlag, Berlin.
- (2) Obinger, C. (2010) Heme peroxidase biochemistry: Facts and perspectives. *Arch. Biochem. Biophys.* 500, 1–2.
- (3) Zamocky, M., Jakopitsch, C., Furtmüller, P.G., Dunand, C., and Obinger, C. (2008) The peroxidase-cyclooxygenase superfamily. Reconstructed evolution of critical enzymes of the innate immune system. *Proteins* 71, 589–605.
- (4) Davies, M. J., Hawkins, C. L., Pattison, D. I., and Rees, M. D. (2008) Mammalian heme peroxidases: From molecular mechanisms to health implications. *Antioxid. Redox Signaling* 10, 1199–1234.
- (5) Arnhold, J., and Flemming, J. (2010) Human myeloperoxidase in innate and acquired immunity. *Arch. Biochem. Biophys.* 500, 92–106.
- (6) Furtmüller, P. G., Zederbauer, M., Jantschko, W., Helm, J., Bogner, M., Jakopitsch, C., and Obinger, C. (2006) Active site structure and catalytic mechanisms of human peroxidases. *Arch. Biochem. Biophys.* 445, 199–213.
- (7) Zederbauer, M., Furtmüller, P. G., Brogioni, S., Jakopitsch, C., Smulevich, G., and Obinger, C. (2007) Heme to protein linkages in mammalian peroxidases: Impact on spectroscopic, redox and catalytic properties. *Nat. Prod. Rep.* 24, 571–584.
- (8) Fiedler, T. J., Davey, C. A., and Fenna, R. E. (2000) X-ray crystal structure and characterization of halide-binding sites of human myeloperoxidase at 1.8 Å resolution. *J. Biol. Chem.* 275, 11964–11971.
- (9) Carpena, X., Vidossich, P., Schroettner, K., Calisto, B. M., Banerjee, S., Stampl, J., Soudi, M., Furtmüller, P. G., Rovira, I., and Obinger, C. (2009) Essential role of proximal histidine-asparagine interaction in mammalian peroxidases. *J. Biol. Chem.* 284, 25929–25937.
- (10) Singh, A. K., Singh, N., Sharma, S., Singh, S. B., Kaur, P., Bhushan, A., Srinivasan, A., and Singh, T. P. (2008) Crystal structure of lactoperoxidase at 2.4 Å resolution. *J. Mol. Biol.* 376, 1060–1075.
- (11) Oxvig, C., Thomsen, A. R., Overgaard, M. T., Sorensen, P., Hojrup, P., Bjerrum, M. J., Gleich, L., and Sottrup-Jensen, L. (1999) Biochemical evidence for heme linkage through esters with Asp-93 and Glu-241 in human eosinophil peroxidase. The ester with Asp-93 is only partially formed *in vivo*. *J. Biol. Chem.* 274, 16953–16958.
- (12) DePillis, G. D., Ozaki, S., Kuo, J. M., Maltby, D. A., and Ortiz de Montellano, P. R. (1997) Autocatalytic processing of heme by lactoperoxidase produces the native protein-bound prosthetic group. *J. Biol. Chem.* 272, 8857–8860.

- (13) Fayadat, L., Niccoli-Sire, P., Lanet, J., and Franc, J. L. (1999) Role of heme in intracellular trafficking of thyroperoxidase and involvement of  $\text{H}_2\text{O}_2$  generated at the apical surface of thyroid cells in autocatalytic covalent heme binding. *J. Biol. Chem.* 274, 10533–10538.
- (14) Ortiz de Montellano, P. R. (2008) Mechanism and role of covalent heme binding in the CYP4 family of P450 enzymes and the mammalian peroxidases. *Drug Metab. Rev.* 40, 405–426.
- (15) Huang, L., Wojciechowski, G., and Ortiz de Montellano, P. R. (2006) Role of heme-protein covalent bonds in mammalian peroxidases. Protection of the heme by a single engineered heme-protein link in horseradish peroxidase. *J. Biol. Chem.* 281, 18983–18988.
- (16) Huang, L., and Ortiz de Montellano, P. R. (2006) Heme-protein covalent bonds in peroxidases and resistance to heme modification during halide oxidation. *Arch. Biochem. Biophys.* 446, 77–83.
- (17) Andrews, P. C., and Krinsky, N. I. (1981) The reductive cleavage of myeloperoxidase in half, producing enzymically active hemi-myeloperoxidase. *J. Biol. Chem.* 256, 4211–4218.
- (18) Weber, R., and Plat, H. (1981) Spectral properties of myeloperoxidase and its ligand complexes. *Biochim. Biophys. Acta* 661, 235–239.
- (19) Brogioni, S., Feis, A., Marzocchi, M. P., Zederbauer, M., Furtmüller, P. G., Obinger, C., and Smulevich, G. (2006) Resonance Raman assignment of myeloperoxidase and the selected mutants Asp94Val and Met243Thr. *J. Raman Spectrosc.* 37, 263–276.
- (20) Brogioni, S., Stampl, J., Furtmüller, P. G., Feis, A., Obinger, C., and Smulevich, G. (2008) The role of the sulfonium linkage in the stabilization of the ferrous form of myeloperoxidase: A comparison with lactoperoxidase. *Biochim. Biophys. Acta* 1784, 843–849.
- (21) Arnhold, J., Monzani, E., Furtmüller, P. G., Zederbauer, M., Casella, L., and Obinger, C. (2006) Kinetics and thermodynamics of halide and nitrite oxidation by mammalian heme peroxidases. *Eur. J. Inorg. Chem.*, 3801–3811.
- (22) Battistuzzi, G., Bellei, M., Vlasits, J., Banerjee, S., Furtmüller, P. G., Sola, M., and Obinger, C. (2010) Redox thermodynamics of lactoperoxidase and eosinophil peroxidase. *Arch. Biochem. Biophys.* 494, 72–77.
- (23) Battistuzzi, G., Bellei, M., Zederbauer, M., Furtmüller, P. G., Sola, M., and Obinger, C. (2006) Redox thermodynamics of the Fe(III)/Fe(II) couple of human myeloperoxidase in its high-spin and low-spin forms. *Biochemistry* 45, 12750–12755.
- (24) Kooter, I. M., Moguilevsky, N., Bollen, A., Sijtsma, N. M., Otto, C., and Weber, R. (1997) Site-directed mutagenesis of Met243, a residue of myeloperoxidase involved in binding of the prosthetic group. *J. Biol. Inorg. Chem.* 2, 191–197.
- (25) Zederbauer, M., Furtmüller, P. G., Ganster, B., Moguilevsky, N., and Obinger, C. (2007) The vinyl-sulfonium bond in human myeloperoxidase: Impact on compound I formation and reduction by halides and thiocyanate. *Biochem. Biophys. Res. Commun.* 356, 450–456.
- (26) Zederbauer, M., Jantschko, W., Neugschwandtner, K., Jakopitsch, C., Moguilevsky, N., Obinger, C., and Furtmüller, P. G. (2005) Role of the covalent glutamic acid 242–heme linkage in the formation and reactivity of redox intermediates of human myeloperoxidase. *Biochemistry* 44, 6482–6491.
- (27) Zederbauer, M., Furtmüller, P. G., Bellei, M., Stampl, J., Jakopitsch, C., Battistuzzi, G., Moguilevsky, N., and Obinger, C. (2007) Disruption of the aspartate to heme ester linkage in human myeloperoxidase. Impact on ligand binding, redox chemistry, and interconversion of redox intermediates. *J. Biol. Chem.* 282, 17041–17052.
- (28) Moguilevsky, N., Garcia-Quintana, L., Jacquet, A., Tournay, L., Fabry, L., Pierard, L., and Bollen, A. (1991) Structural and biological properties of human recombinant myeloperoxidase produced by Chinese hamster ovary cell lines. *Eur. J. Biochem.* 197, 605–614.
- (29) Odajima, T., and Yamazaki, I. (1970) Myeloperoxidase of the leukocyte of normal blood. I. Reaction of myeloperoxidase with hydrogen peroxide. *Biochim. Biophys. Acta* 206, 71–74.

- (30) Battistuzzi, G., Bellei, M., Borsari, M., Di Rocco, G., Ranieri, A., and Sola, M. (2005) Axial ligation and polypeptide matrix effects on the reduction potential of heme proteins probed on their cyanide adducts. *J. Biol. Inorg. Chem.* 10, 643–651.
- (31) Bellei, M., Battistuzzi, G., Jakopitsch, C., Sola, M., and Obinger, C. (2006) Redox thermodynamics of the ferric-ferrous couple of wild-type *Synechocystis* KatG and KatG(Y249F). *Biochemistry* 45, 4768–4774.
- (32) Battistuzzi, G., Bellei, M., De Rienzo, F., and Sola, M. (2006) Redox properties of the  $\text{Fe}^{3+}/\text{Fe}^{2+}$  couple in *Arthromyces ramosus* class II peroxidase and its cyanide adduct. *J. Biol. Inorg. Chem.* 11, 586–532.
- (33) Yee, E. L., Cave, R. J., Guyer, K. L., Tyma, P. D., and Weaver, M. J. (1979) A survey of ligand effects upon the reaction entropies of some transition metal redox couples. *J. Am. Chem. Soc.* 101, 1131–1137.
- (34) Battistuzzi, G., Borsari, M., Ranieri, A., and Sola, M. (2002) Redox thermodynamics of the  $\text{Fe}^{3+}/\text{Fe}^{2+}$  couple in horseradish peroxidase and its cyanide complex. *J. Am. Chem. Soc.* 124, 26–27.
- (35) Battistuzzi, G., Borsari, M., Cowan, J. A., Ranieri, A., and Sola, M. (2002) Control of cytochrome *c* redox potential: Axial ligation and protein environment effects. *J. Am. Chem. Soc.* 124, 5315–5324.
- (36) Battistuzzi, G., Bellei, M., Bortolotti, C. A., and Sola, M. (2010) Redox properties of heme peroxidases. *Arch. Biochem. Biophys.* 500, 21–36.
- (37) Olea, C., Boon, E. M., Pellicena, P., Kuriyan, J., and Marletta, M. A. (2008) Probing the function of heme distortion in the H-NOX family. *ACS Chem. Biol.* 3, 703–710.
- (38) Olea, C., Kuriyan, J., and Marletta, M. A. (2010) Modulating heme redox potential through protein-induced porphyrin distortion. *J. Am. Chem. Soc.* 132, 1294–12795.
- (39) Takano, Y., and Nakamura, H. (2009) Density functional study of roles of porphyrin ring in electronic structure of heme. *Int. J. Quantum Chem.* 109, 3583–3591.
- (40) Shokhireva, T. K., Berry, R. E., Uno, E., Balfour, C. A., Zhang, H., and Walker, F. A. (2003) Electrochemical and NMR spectroscopic studies of distal pocket mutants of nitrophorin 2: Stability, structure, and dynamics of axial ligand complexes. *Proc. Natl. Acad. Sci. U.S.A.* 100, 3778–3783.
- (41) Ma, J. G., Zhang, J., Franco, R., Jia, S. L., Moura, I., Moura, J. J., Kroneck, P. M., and Shelnutt, J. A. (1998) The structural origin of nonplanar heme distortions in tetraheme ferricytochromes  $c_3$ . *Biochemistry* 37, 12431–12442.
- (42) Shelnutt, J. A., Song, X. Z., Ma, J. G., Jia, S. L., Jentzen, W., and Medforth, C. J. (1998) Non planar porphyrins and their significance in proteins. *Chem. Soc. Rev.* 27, 31–41.
- (43) Furtmüller, P. G., Jantschko, W., Regelsberger, G., Jakopitsch, C., Moguilevsky, N., and Obinger, C. (2001) A transient kinetic study on the reactivity of recombinant unprocessed monomeric myeloperoxidase. *FEBS Lett.* 503, 147–150.
- (44) Van Antwerpen, P., Slomianny, M.-C., Zouaoui Boudjeltia, K., Delporte, C., Faid, V., Calay, D., Rousseau, A., Moguilevsky, N., Raes, M., Vanhamme, L., Furtmüller, P. G., Obinger, C., Vanheesbeek, M., Neve, J., and Michalski, J.-C. (2010) Glycosylation pattern of mature dimeric leukocyte and recombinant monomeric myeloperoxidase: Glycosylation is required for optimal enzymatic activity. *J. Biol. Chem.* 285, 16351–16359.
- (45) Banerjee, S., Stamper, J., Furtmüller, P.G., and Obinger, C. (2011) Conformational and thermal stability of mature dimeric human myeloperoxidase and a recombinant form from CHO cells. *Biochim. Biophys. Acta* 1814, 375–387.
- (46) Nauseef, W. M., McCormick, H., and Yi, H. (1992) Roles of heme insertion and the mannose-6-phosphate receptor in processing of the human myeloid lysosomal enzyme, myeloperoxidase. *Blood* 80, 2622–2633.
- (47) Hansson, M., Olsson, I., and Nauseef, W. M. (2006) Biosynthesis, processing, and sorting of human myeloperoxidase. *Arch. Biochem. Biophys.* 445, 214–224.
- (48) Arnhold, J., Furtmüller, P., and Obinger, C. (2003) Redox properties of myeloperoxidase. *Redox Rep.* 8, 179–186.
- (49) Furtmüller, P. G., Arnhold, J., Jantschko, W., Pichler, H., and Obinger, C. (2003) Redox properties of the couples compound I/compound II and compound II/native enzyme of human myeloperoxidase. *Biochem. Biophys. Res. Commun.* 301, 551–557.
- (50) Devarajan, A., Gaenko, A. V., and Ryde, U. (2008) Effect of covalent links on the structure, spectra, and redox properties of myeloperoxidase: A density functional study. *J. Inorg. Biochem.* 102, 1549–15557.